

Title	The use of inline high-shear rotor-stator mixing for preparation of high-solids milk-protein-stabilised oil-in-water emulsions with different protein:fat ratios
Authors	O'Sullivan, Jonathan J.;Drapala, Kamil P.;Kelly, Alan L.;O'Mahony, James A.
Publication date	2017-09-27
Original Citation	O'Sullivan, J. J., Drapala, K. P., Kelly, A. L. and O'Mahony, J. A. (2017) 'The use of inline high-shear rotor-stator mixing for preparation of high-solids milk-protein-stabilised oil-in-water emulsions with different protein:fat ratios', Journal of Food Engineering, In Press. doi:10.1016/j.jfoodeng.2017.10.015
Type of publication	Article (peer-reviewed)
Link to publisher's version	http://www.sciencedirect.com/science/article/pii/S0260877417304466 - 10.1016/j.jfoodeng.2017.10.015
Rights	© 2017 Elsevier Ltd. This manuscript version is made available under the CC-BY-NC-ND 4.0 license. - http://creativecommons.org/licenses/by-nc-nd/4.0/
Download date	2025-04-29 14:41:19
Item downloaded from	https://hdl.handle.net/10468/4999



UCC

University College Cork, Ireland
Coláiste na hOllscoile Corcaigh

Accepted Manuscript

The use of inline high-shear rotor-stator mixing for preparation of high-solids milk-protein-stabilised oil-in-water emulsions with different protein:fat ratios

Jonathan J. O'Sullivan, Kamil P. Drapala, Alan L. Kelly, James A. O'Mahony



PII: S0260-8774(17)30446-6
DOI: 10.1016/j.jfoodeng.2017.10.015
Reference: JFOE 9048
To appear in: *Journal of Food Engineering*
Received Date: 09 August 2017
Revised Date: 17 October 2017
Accepted Date: 22 October 2017

Please cite this article as: Jonathan J. O'Sullivan, Kamil P. Drapala, Alan L. Kelly, James A. O'Mahony, The use of inline high-shear rotor-stator mixing for preparation of high-solids milk-protein-stabilised oil-in-water emulsions with different protein:fat ratios, *Journal of Food Engineering* (2017), doi: 10.1016/j.jfoodeng.2017.10.015

This is a PDF file of an unedited manuscript that has been accepted for publication. As a service to our customers we are providing this early version of the manuscript. The manuscript will undergo copyediting, typesetting, and review of the resulting proof before it is published in its final form. Please note that during the production process errors may be discovered which could affect the content, and all legal disclaimers that apply to the journal pertain.

Highlights

- Emulsification of different fat-filled milk formulations was investigated.
- Emulsification was achieved using novel inline high-shear mixing technology.
- The emulsification process was monitored inline using pressure drop analysis.
- Pressure drop data allowed for the estimation of viscosity during emulsion formation.

1 **The use of inline high-shear rotor-stator mixing for preparation of high-solids milk-**
2 **protein-stabilised oil-in-water emulsions with different protein:fat ratios**

3

4 Jonathan J. O'Sullivan^{a,b}, Kamil P. Drapala^{a,b}, Alan L. Kelly^{a,b}, James A. O'Mahony^{a,b*}

5

6 ^aSchool of Food and Nutritional Sciences, University College Cork, Cork, Ireland

7 ^bDairy Processing Technology Centre, University College Cork, Cork, Ireland

8

9 * Corresponding author: Email address: sa.omahony@ucc.ie

10 **Abstract:**

11 The emulsification of refined palm oil (RPO) in a continuous phase consisting of skim milk
12 concentrate (SMC) and maltodextrin with a dextrose equivalent value of 17 (MD17) to produce
13 fat-filled milk emulsions (FFMEs), was studied. A novel inline high-shear mixing (IHSM)
14 method was used to produce emulsions, and three protein contents were investigated at a fixed
15 RPO content of 12%: low (7.7%), medium (10.5%) and high (13%). Pressure drop
16 measurement was used as an inline approach to determine viscosity using the Hagen-Poiseuille
17 equation. In addition, offline viscometry, particle size and emulsion stability analyses were
18 performed. Emulsion fat droplet size decreased significantly ($P < 0.05$) as a function of number
19 of passes through the IHSM, due to an effective increase in residence time. Furthermore, inline
20 pressure drop data demonstrated that the emulsification process displayed two distinct stages:
21 (i) oil injection, and (ii) reduction in fat droplet size, irrespective of protein content.

22

23 **Keywords:** High solids emulsions, High-shear inline mixer, Pressure drop, Skim milk
24 concentrate, Refined palm oil, Maltodextrin

25 1. Introduction

26 Milk is a highly versatile raw material and, over the past century, significant advances
27 have been achieved in its fractionation into a wide variety of components (Fox, 2008;
28 O'Sullivan & O'Mahony, 2016). These constituent-based ingredients are often recombined,
29 sometimes with ingredients derived from other sources (*e.g.*, plant-derived proteins,
30 carbohydrates and lipids), to achieve different formulations, which can be utilised as final
31 products by the consumer (*e.g.*, enriched milk powders), or be further processed as ingredients
32 by food manufacturers (*e.g.*, protein concentrates/isolates or blends, for example in the
33 manufacture of infant formulae) (O'Connell & Flynn, 2007). One such example is fat-filled
34 milk powders (FFMPs), which are dried protein-stabilised emulsions, typically produced by
35 solids concentration (*e.g.*, by evaporation) and homogenisation followed by spray drying.
36 These systems are intended either for direct reconstitution by consumers, or as ingredients in a
37 variety of recombined applications, such as beverages, ice cream, confectionary and bakery
38 products (Sharma *et al.*, 2012; Vignolles *et al.*, 2007).

39 The formulation of these fat-filled milk emulsions (FFMEs) prior to spray-drying
40 typically involves blending of skim milk concentrate (SMC; *i.e.*, a concentrated protein and
41 lactose solution) with oils (*i.e.*, often derived from plants, such as coconut or palm oils) to
42 achieve the required ratio of protein to fat, and with additional carbohydrates added (Sharma
43 *et al.*, 2012). SMC is produced by removal of the fat from milk through centrifugation and
44 concentrating the remaining stream to a solids content of >35% (w/w) (O'Connell & Flynn,
45 2007). FFMEs are typically prepared by injecting fats into SMC, followed by emulsification
46 using two-stage valve homogenisation. The fats that are used are typically derived from plants
47 and are either solid or semi-solid at ambient temperature, in order to be comparable to milk fat.
48 Thus, prior to injection, these fats need to be liquefied and dosed into the SMC at elevated
49 temperatures, in the range 50-60°C usually (Vignolles *et al.*, 2007). The ratio of protein with

50 respect to a fixed fat content is influenced by addition of carbohydrates (which reduces the
51 protein content), often maltodextrins; these are polysaccharides of variable chain length
52 produced by partial hydrolysis of starch, which are defined by their dextrose equivalent (DE)
53 value (Drapala *et al.*, 2016; Mulcahy *et al.*, 2016; O'Mahony *et al.*, 2017). Use of higher
54 concentrations of protein (*e.g.*, >5% w/w) in emulsion systems, in comparison to lower
55 concentrations of protein, yields smaller emulsion droplets which are more resistant to
56 emulsion instability, due to greater coverage of the droplet interface, reducing the propensity
57 towards coalescence and increasing the electrostatic repulsive interactions between protein-
58 stabilised emulsion droplets (O'Sullivan *et al.*, 2014; O'Sullivan, Park, & Beevers, 2016).
59 Furthermore, dairy-derived carbohydrate sources, such as lactose or permeate from
60 ultrafiltration of skim milk, are widely employed to vary the protein content with respect to fat
61 in a similar fashion to maltodextrin addition. Plant-derived oils and maltodextrin ingredients
62 are commonly used owing to their lower overall cost and reduced powder stickiness challenges
63 during spray-drying, respectively (Gonzalez-Perez & Arellano, 2009; Vega & Roos, 2006).

64 After oil injection and emulsification, these formulations are spray-dried to yield FFMP
65 (Sharma *et al.*, 2012). To the authors' knowledge, there are no studies available in the published
66 literature detailing the formation of these high solids emulsion systems, the role of protein-to-
67 fat ratio in their formation and stability, and the inline monitoring of this process from fat
68 injection through to formation of the final emulsion. This study aims to investigate the emulsion
69 formation process for high solids emulsions, using an inline high-shear mixer (IHSM) for
70 emulsification, in a recirculation configuration (*i.e.*, semi-continuous), and to assess the
71 suitability of using a pressure drop approach to monitor the process in real-time, from fat
72 injection through to final emulsion formation.

73 High-shear mixers are widely used for emulsification applications and the dissolution
74 of powders to form homogeneous solutions (Hall *et al.*, 2013; O'Sullivan *et al.*, 2017). The

75 configuration of these mixers is that of a rotor-stator, and they can be used in an inline
76 configuration for either continuous processing (*i.e.*, single-pass mode) or semi-continuous
77 processing (*i.e.*, multiple-pass mode), and are highly energy efficient (Hall *et al.*, 2011). The
78 shear rate range for high-shear mixers is typically within the range 20,000 – 100,000 s⁻¹,
79 depending on factors such as tip speed, rotor-stator geometry (*e.g.*, single or double screen)
80 and physical properties (*e.g.*, viscosity, presence of particulates, etc.) of the material being
81 processed (Pacek *et al.*, 2007). Pressure drop across a section of pipeline, for a flowing fluid,
82 can be measured using a pair of pressure transducers, separated by a known distance. Pressure
83 drop data provides useful information as to how a process is performing in real-time, as the
84 data can be used to calculate a theoretical viscosity value from the Hagen-Poiseuille equation
85 (Douglas *et al.*, 2005; Mihailova *et al.*, 2015). O’Sullivan *et al.* (2017) demonstrated the
86 suitability of a pressure drop approach for monitoring the induction of dairy powders in real-
87 time, observing different aspects of the process, such as initial contact of the powder with water,
88 and the disintegration of powder particles as a function of processing time.

89 The overall objective of this research was to evaluate the suitability of the IHSM
90 technology and discern differences in emulsification behaviour based on FFME formulation,
91 in terms of emulsion fat droplet size distribution, emulsion viscosity and accelerated physical
92 stability, as a function of processing time. Moreover, the emulsification process was monitored
93 inline using a pressure drop approach, by applying the Hagen-Poiseuille equation. This
94 approach allows for real-time monitoring of industrial emulsification processes, and provides
95 information as to when dosing of oils is complete, as well as the progression of the
96 emulsification process.

97 **2. Materials and methods**

98 *2.1. Materials*

99 Skim milk concentrate (SMC) and refined palm oil (RPO) were kindly provided by
100 Dairygold Food Ingredients (Mitchelstown, Ireland). Maltodextrin with a dextrose equivalent
101 (DE) value of 17 (MD17) was supplied by Corcoran Chemicals Ltd. (Dublin, Ireland). The
102 composition of the SMC is presented in Table 1. The water used throughout this study was
103 deionised water, unless stated otherwise.

104 2.2. Emulsion formulation and preparation

105 Emulsification was conducted at three protein concentrations, 7.7, 10.5 and 13% (w/w),
106 with a fixed fat content of $12.1 \pm 0.1\%$ (w/w), whereby the % (w/w) level is based on total
107 solids within a given system (*i.e.*, formulated emulsion or projected FFMP). Variations in
108 emulsion formulation to meet these protein concentrations were achieved through addition of
109 a fixed quantity of RPO and varying quantities of MD17 and water to SMC, as detailed in
110 Table 1, with a target solids content of $52.3 \pm 0.2\%$ (w/w) in all cases. These protein contents
111 were selected as the range in protein content for typical FFMP products is 14 to 24% (w/w) for
112 the low to high protein contents, respectively (Sharma *et al.*, 2012). The predicted protein
113 content of powders produced from the prepared emulsions would be 14.2, 19.2 and 23.7%
114 (w/w) for the low-, medium- and high-protein systems, respectively, assuming that the final
115 moisture content of the powder was 4% (w/w) in all cases (Table 1).

116 The configuration used for emulsification is shown in Fig. 1. The emulsification process
117 was started by filling the closed-loop liquid system with the required amount of SMC to achieve
118 the desired protein content for the investigated emulsion systems (Table 1), and initialising the
119 progressive cavity pump (Torqueflow, Sydex, UK) at a volumetric flowrate of 675 L h^{-1} . Next,
120 the inline high-shear mixer (IHSM), a YTRON-Z (1.50FC, YTRON Process Technology
121 GmbH, Germany) operating at 100% capacity, yielding *ca.* 6,000 rpm, was initialised, and the
122 custom-fabricated heat exchanger (Liam A. Barry Ltd., Cork, Ireland), in counter-current

123 configuration, was set to a temperature of 50°C. An overhead stirrer (RZR 2021, Heidolph
124 Instruments GmbH & Co. KG, Schwabach, Germany) at a speed of 1,000 rpm was used to
125 ensure rapid dispersion of MD17 powder and added water, and retained in place for the duration
126 of the emulsification process. The required mass of MD17 and water were carefully added to
127 the feed vessel over the top once the temperature of the recirculating SMC had reached 50°C
128 and the mixture was allowed to circulate through the system for a minimum of 30 min.
129 Subsequently, RPO was liquefied at a temperature of 50°C, the required mass was added to the
130 feed vessel over the top, and the mix was emulsified for up to 15 min (>50 passes through the
131 IHSM).

132 2.3. Emulsion droplet size characterisation

133 The changes in fat droplet size as a function of pass number (1, 3, 5, 10, 25 and 50
134 passes) through the IHSM were measured by static light-scattering using a Mastersizer 3000
135 (Hydro EV, Malvern Instruments, UK). Emulsion fat droplet size was reported as $d_{4,3}$ (*i.e.*,
136 volume-weighted mean droplet size), d_{10} (*i.e.*, cumulative 10% point of diameter), d_{50} (*i.e.*,
137 cumulative 50% point of diameter), d_{90} (*i.e.*, cumulative 90% point of diameter), droplet size
138 distribution data (DSD; volume vs. size class), and span (*i.e.*, width of the droplet size
139 distribution). *Eq. 1* was used in order to determine the times required to achieve the desired
140 number of passes of the emulsion through the IHSM (O'Sullivan *et al.*, 2015):

$$141 \quad t = \frac{V \times \text{Pass number}}{Q} \quad (1)$$

142 where t is the residence time (s), V is the volume within the system (m³), and Q is the volumetric
143 flow rate (m³ s⁻¹).

144 2.4. Viscosity determination: comparison of calculated and experimental approaches

145 Viscosity was calculated from experimentally measured pressure drop (ΔP) readings,
 146 and compared to experimentally measured viscosity, in order to validate the calculated
 147 viscosity results, using a similar approach to that described by O’Sullivan *et al.* (2017).
 148 Pressure drop was recorded for the emulsification process, at all protein:fat ratios, and was
 149 recorded using a pair of pressure transducers (PR-33X, Keller, UK), positioned 1.08 m apart
 150 (Fig. 1). Pressure differential data was collected before dosage of molten RPO and for up to 15
 151 min during the emulsification process. Calculated viscosity values were determined from Eq.
 152 2, the Hagen-Poiseuille equation, using experimentally-measured pressure drop values, as
 153 follows (Douglas *et al.*, 2005; O’Sullivan *et al.*, 2017):

$$154 \quad \eta_{\text{calculated}} = \frac{\pi \Delta P d^4}{128 L Q} \quad (2)$$

155 where $\eta_{\text{calculated}}$ is the calculated viscosity (Pa.s), ΔP is the pressure differential across a given
 156 straight section of pipeline (Pa), d is the internal diameter (19.05 mm), L is the length over
 157 which the pressure drop was recorded (1.08 m), and Q is the volumetric flow rate ($\text{m}^3 \text{s}^{-1}$).

158 The experimental viscosity ($\eta_{\text{experimental}}$) was measured for all emulsion systems, after 1
 159 and 50 passes, using a rotational viscometer (RST-CC Touch™, Brookfield AMETEK,
 160 Middleboro, MA, USA) equipped with a cup-and-bob geometry. Apparent viscosity was
 161 measured at 50°C (*i.e.*, the mean temperature at which emulsification was conducted; Section
 162 2.2). A shear rate of 300 s^{-1} was used for viscosity determination, as this was determined to be
 163 similar to the shear rate in the pipeline between the pair of pressure transducers; the calculated
 164 shear rate within the 1.08 m section from which the pressure drop was recorded was 275 s^{-1} ,
 165 determined using Eq. 3 (Douglas *et al.*, 2005):

$$166 \quad \dot{\gamma} = \frac{8v}{d}, \text{ where } v = \frac{Q}{A} \quad (3)$$

167 where $\dot{\gamma}$ is the shear rate (s^{-1}), d is the internal diameter (19.05 mm), v is the average velocity
168 (m s^{-1}), Q is the volumetric flowrate (m^3s^{-1}), and A is the cross-sectional area (m^2).

169 2.5. Accelerated physical stability analysis of emulsions

170 Separation rates of FFMEs collected after 1 and 50 passes of aqueous and oil phases
171 through the IHSM were measured using an analytical centrifuge (LUMiSizer, L.U.M. GmbH,
172 Berlin, Germany). The principle of analysis by LUMiSizer has been detailed by Lerche and
173 Sobisch (2011). Stability of emulsions to separation (i.e., creaming and sedimentation) driven
174 by difference in the density between fat globules, undissolved powder and protein aggregates
175 and the aqueous phase was determined at 23°C and 563 g over 500 min (i.e., 8 h 20 min) as
176 detailed by Shimoni *et al.* (2013). Separation rates were calculated from integral transmission
177 (IT) profiles using the initial linear ($R^2 \geq 0.95$) region of the slope of the plot of integral
178 transmission *vs.* measurement time. Separation profiles (i.e., the Space- and Time-resolved
179 Extinction Profiles, STEP; Lerche and Sobisch, 2011) were collected at 10 min intervals during
180 accelerated testing of emulsions to give information on changes in the light transmission
181 through the measurement cell as a function of the specific position in the cell and, effectively,
182 indicating progressive migration of emulsion components (i.e., creaming and/or
183 sedimentation).

184 2.6. Statistical analysis

185 Presented data are the average and standard deviation of at least three repeat
186 measurements, and from a single production run of SMC, RPO and MD17. Student's t-test
187 with a 95% confidence interval analysis was performed using Microsoft Excel and was used to
188 assess the significance of the results obtained, whereby t-test differences with $P < 0.05$ were
189 considered statistically significant.

190 3. Results and discussion

191 3.1. Effect of pass number through the inline high-shear mixer (IHSM) on fat droplet size 192 distribution

193 The effect of pass number through the IHSM (*i.e.*, residence time within the shear field)
194 on fat droplet size distribution was assessed for low-, medium- and high-protein FFMEs (Fig.
195 2 and Table 2). After a single pass through the IHSM, large fat droplets were found; the
196 medium-protein FFME yielded the smallest initial droplets ($d_{4,3}$ of $6.67 \pm 0.31 \mu\text{m}$), while the
197 high-protein FFME yielded the largest initial droplet size ($d_{4,3}$ of $9.62 \pm 0.79 \mu\text{m}$). This may
198 be explained by the fact that moderate concentrations of protein allow for more efficient
199 adsorption and stabilisation of oil-water interfacial layers, yielding smaller emulsion droplets
200 (Beverung *et al.*, 1999; O'Sullivan, Beevers *et al.*, 2015). As these samples were further
201 processed (*i.e.*, with increasing pass number), the size of the fat droplets (in particular d_{50} and
202 d_{90} ; Table 2) decreased significantly ($P < 0.05$), for all protein contents investigated.

203 Furthermore, the extent of droplet size reduction was greatest for the low-protein
204 emulsions, in terms of d_{50} and d_{90} , throughout the entire process. This behaviour was attributed
205 to the higher viscosity of the continuous phase of those systems in comparison to that of the
206 medium- and high-protein samples, allowing for greater ease of disruption of fat droplets (Lee
207 *et al.*, 2013; Walstra, 1993). A higher viscosity difference between the continuous and
208 dispersed phases (*i.e.*, viscosity ratio), results in enhanced droplet breakup within the turbulent
209 flow regimes observed for the IHSM (Walstra & Smulders, 2000). Furthermore, the primary
210 mode of droplet breakup within the IHSM results from the high degree of turbulence, which
211 causes chaotic velocity fields, resulting in turbulent eddies, characterised by the Kolmogorov
212 length scale (Walstra, 1993).

213 In addition, in all cases, and for any given time point in the process, a bimodal size
214 distribution was observed (Fig. 2), in which the micron-sized peak (*ca.* 5 μm after 50 passes)
215 was ascribed to emulsion fat droplets, whereas the submicron peak (*ca.* 250 nm) was associated
216 with casein micelles, the dominant protein fraction of SMC (O'Sullivan *et al.*, 2017). After 25
217 passes through the IHSM, the low-protein (7.7% w/w) emulsion had droplets $\leq 10 \mu\text{m}$ (Fig.
218 2a), while droplets $> 10 \mu\text{m}$ were still present in the medium- (Fig. 2b) and high-protein (Fig.
219 2c) emulsions even after 50 passes through the IHSM. It is also worth noting that the low-
220 protein emulsion had the narrowest droplet size distribution (DSD; Fig. 2a), irrespective of the
221 number of passes through the IHSM, as also evident from the lowest span values for this
222 emulsion (Table 2), compared to medium- and high-protein emulsions. This is thought to be
223 associated with the higher viscosity of the continuous phase of the low-protein content FFME,
224 in comparison to the other protein contents. The reduction of emulsion droplet size as a function
225 of pass number was similarly demonstrated for a range of other emulsification processes,
226 including IHSMs (Hall *et al.*, 2011), continuous ultrasonic processors (O'Sullivan *et al.*, 2015),
227 high-pressure valve homogenisers (Lee & Norton, 2013) and microfluidizers (Lee & Norton,
228 2013).

229 3.2. *Inline assessment of emulsification using the pressure drop approach*

230 The calculated viscosity ($\eta_{\text{calculated}}$) as a function of pass number (up to 50 passes) was
231 investigated and is shown in Fig. 3 for FFMEs prepared at low-, medium- and high-protein
232 concentrations. Upon addition of molten RPO to the emulsification system (Fig. 1), there was
233 a significant increase ($P < 0.05$) in $\eta_{\text{calculated}}$ for all of the investigated formulations, where this
234 behaviour was ascribed to the increased solids content within the system, resulting in an
235 increased pressure differential and thus $\eta_{\text{calculated}}$ (Douglas *et al.*, 2005; O'Sullivan *et al.*, 2017).
236 Following the addition of fat, $\eta_{\text{calculated}}$ decreased marginally as a function of pass number, in
237 particular for the medium-protein FFME. This behaviour was attributed to the reduction of fat

238 droplet size, which is known to result in a reduced viscosity for emulsion systems
239 (McClements, 2005). Thus, the emulsification process exhibited two distinct stages in all
240 instances, an initial significant ($P < 0.05$) increase, followed by a gradual reduction to a final
241 viscosity value. These distinct stages correspond to: (i) an increase in the solids content of the
242 system due to the introduction of molten fat to the skim milk concentrate (SMC), and (ii) size
243 reduction of fat droplets with successive passes through the IHSM.

244 Furthermore, when comparing $\eta_{calculated}$ values after 50 passes for each FFME
245 formulation, the low-protein emulsion exhibited, unexpectedly, the highest viscosity value
246 (36.5 ± 1.3 mPa.s), followed by the high-protein emulsion, with a marginally lower viscosity
247 value (34.7 ± 2.2 mPa.s), and the medium-protein sample, which had a significantly lower (P
248 < 0.05) viscosity (29.2 ± 0.7 mPa.s), in comparison to both the low- and high-protein systems.
249 Even though all of the systems had the same solids content (52.5% w/w; Table 1), the factor
250 which dictated the resultant value of $\eta_{calculated}$ was thought to be the concentration of MD17,
251 rather than the protein content. MD17 has an average molecular weight of 24.9 kDa (Chen &
252 O'Mahony, 2016; Rong *et al.*, 2009), and maltodextrin has a highly branched structure
253 consisting of D-glucose monomer units (Avaltroni *et al.*, 2004; Chronakis, 1998; Wang &
254 Wang, 2000); in addition, individual molecules of MD17 interact with one another,
255 contributing to increases in viscosity with increasing concentration (Avaltroni *et al.*, 2004;
256 Morris *et al.*, 1981). The intrinsic viscosity ($[\eta]$; *i.e.*, hydrodynamic volume) of MD17 is
257 significantly greater than that of the proteins in SMC, *ca.* 80:20 mixture of casein micelles and
258 whey protein, the same as observed in milk protein isolates (MPI) (O'Connell & Flynn, 2007;
259 Vos *et al.*, 2016), whereby the $[\eta]_{MD17}$ was 3.5 dL g⁻¹, in comparison to $[\eta]_{MPI}$ which had a
260 value of 0.59 dL g⁻¹ (Avaltroni *et al.*, 2004; O'Sullivan *et al.*, 2014). The significantly ($P <$
261 0.05) higher value of $[\eta]_{MD17}$ highlights that MD17 would have a more pronounced effect on
262 the resultant viscosity of FFMEs than the protein component. Thus, the higher concentration

263 of MD17 in the low-protein content emulsion yielded the highest viscosity and, as the
264 concentration of MD17 decreased, and that of protein increased, there was a significant ($P <$
265 0.05) decrease in viscosity. Moreover, as the concentration of MD17 further decreased, and the
266 concentration of protein increased, the protein component becomes the dominant influencer of
267 viscosity, in comparison to MD17; nevertheless, the resultant viscosity remained lower than
268 that of the low-protein emulsion system (Fig. 3).

269 The validity of the $\eta_{calculated}$ results was assessed through direct comparison of
270 experimentally obtained viscosity values measured at a shear rate of 300 s^{-1} , a value close to
271 that at which the pressure drop was measured (275 s^{-1}), and at the average temperature recorded
272 during emulsification (50°C). The values of $\eta_{calculated}$ and experimental viscosity ($\eta_{experimental}$)
273 for all of the investigated FFME systems, after 1 and 50 passes, are shown in Table 3. The
274 trend of $\eta_{experimental}$ for all of the FFMEs is comparable to that of $\eta_{calculated}$, whereby the low-
275 protein system possessed the highest apparent viscosity and the medium-protein emulsion
276 exhibited the lowest viscosity, for the same reasons as previously discussed, associated with
277 differences in MD17 concentration. Furthermore, the viscosity values for 1 pass were
278 significantly ($P < 0.05$) lower than those at 50 passes, which is in agreement with $\eta_{calculated}$
279 values as a function of time (Fig. 3). This behaviour is ascribed to either the fact that the RPO
280 has not had sufficient time to form a uniform emulsion after a single pass ($< 14\text{ s}$), or potential
281 increased levels of hydration of MD17 resulting from the shearing process.

282 A comparison of the $\eta_{calculated}$ and $\eta_{experimental}$ values for all FFME systems highlight that
283 there is a discrepancy in the values, by a factor of *ca.* 1.25, whereby the calculated value
284 represents an overestimation in all instances. This observed difference between calculated and
285 experimental values was ascribed to the nature of the Hagen-Poiseuille equation, which
286 assumes that the fluid exhibits Newtonian behaviour, whereas it has been established that
287 highly concentrated (52.5% solids, w/w) emulsion systems demonstrate pseudoplastic

288 rheological behaviour (O'Sullivan *et al.*, 2016; Pal, 1996, 2011). A similar trend was observed
289 by O'Sullivan *et al.* (2017) for the induction and dissolution of dairy powders, whereby the
290 difference between calculated and experimental viscosity values was a factor of 2, which was
291 also ascribed to the non-Newtonian behaviour of dairy solutions.

292 3.3. Accelerated physical stability of emulsions

293 Differences in the extent of phase separation in FFME systems after 1 and 50 passes
294 through the IHSM tested under accelerated conditions (563 g for 500 min) were clear from the
295 space- and time-resolved extinction profiles (STEP; Fig. 4). After the 1st pass through the
296 IHSM, only limited differences in phase separation were observed between all emulsions. More
297 pronounced differences in separation were observed for emulsions after 50 passes through the
298 IHSM, where the low-protein (7.7%, w/w) emulsion displayed lowest separation, followed by
299 emulsions with high- (13%, w/w) and medium-protein (10.5%, w/w) levels (Fig. 4). Separation
300 of formulations was identified as being mostly due to the migration of fat globules towards the
301 top of the measuring cell (*i.e.*, creaming) as evidenced by a progressive appearance of a cream
302 layer and only a limited sediment build-up in all samples (Fig. 4). Creaming and sedimentation
303 were reduced on progressive recirculation through the IHSM system, due to decreases in the
304 size of fat globules and enhanced hydration of the MD17 powder (O'Sullivan *et al.*, 2016).

305 Similar emulsion separation trends were observed for the integral transmission (IT)
306 profiles (Fig. 5); the IT represents separation in the samples due to both creaming (upward
307 movement of the less dense phase, *i.e.*, fat droplets, and downward movement of the more
308 dense solutes, *i.e.*, maltodextrin and protein). The evolution of separation increased in the order
309 of low-protein 50th pass < high-protein 50th pass < medium-protein 50th pass < high-protein 1st
310 pass < medium-protein 1st pass < low-protein 1st pass. Despite lack of significant differences
311 in the initial (*i.e.*, first 45 min) slopes of increasing transmission for emulsions after 50 passes

312 through the IHSM (Table 2), the overall (*i.e.*, during 500 min) separation of the low-protein
313 emulsion was lower than that of both medium- and high-protein emulsions after 50 passes (Fig.
314 5). This can be explained by the greater population of smaller particles (*i.e.*, fat globules; Fig.
315 2, Table 2) in the low-protein content emulsion after 50 passes, compared to the other
316 emulsions after 50 passes, causing divergence of the IT profiles after initial movement of the
317 larger particles (*i.e.*, bigger particles move first and smaller particles move more slowly).

318 The results for the accelerated emulsion separation closely correlate with those obtained
319 for DSD and apparent viscosity of the FFME systems, whereas, in accordance with Stoke's
320 Law, emulsions with largest droplet size and lowest viscosity also displayed the most rapid
321 separation. The low-protein emulsion after 50 passes had the highest apparent viscosity,
322 compared to the other emulsions (Table 3), further enhancing stability of the emulsion to
323 density-driven separation.

324 4. Conclusions

325 Inline high-shear mixing (IHSM) was shown to be an effective approach for the
326 preparation of fat-filled milk emulsions (FFMEs). The most effective emulsification, as a
327 function of pass number, was achieved for the low-protein FFME, as observed by the formation
328 of smaller emulsion droplets, which was ascribed to the enhanced droplet breakup due to the
329 increased viscosity differential between the dispersed and continuous phases. Inline
330 measurement of pressure drop is thus an effective approach for monitoring real-time
331 emulsification kinetics of refined palm oil (RPO) in skim milk concentrate (SMC). Pressure
332 drop data was used to determine real-time viscosity, by means of the Hagen-Poiseuille
333 equation; after emulsification, the low-protein FFME exhibited the highest viscosity in
334 comparison to the other systems, which was ascribed to lower and narrower DSD and to the
335 higher content of MD17 and its associated higher intrinsic viscosity in comparison to the

336 protein component of the formulations. The lowest viscosity was exhibited by the medium-
337 protein FFME, associated with the reduction in MD17 concentration. The emulsification
338 process exhibited two distinct phases as observed by pressure drop results: (i) initial injection
339 of fat, and (ii) fat droplet reduction in the shear mixing field.

340

341 **Acknowledgements**

342 The authors would like to acknowledge the Dairy Processing Technology Centre
343 (DPTC), an Enterprise Ireland initiative, for financial support and permission to publish this
344 work. This work was supported by the Irish State through funding from the Technology Centres
345 programme (Grant Number TC/2014/0016). The authors would like to thank Dr Olga
346 Mihailova of Unilever Research (Port Sunlight, UK) for assistance with respect to data
347 processing. The authors would also like to thank Mike Barry and Kevin McEvoy of Liam A.
348 Barry Ltd. (Cork, Ireland) for the custom fabrication of many of the stainless steel components
349 of the experimental setup.

350

351 **References**

352 Avaltroni, F., Bouquerand, P. E., & Normand, V. (2004). Maltodextrin molecular weight
353 distribution influence on the glass transition temperature and viscosity in aqueous
354 solutions. *Carbohydrate Polymers*, 58(3), 323–334.

355 Beverung, C. J., Radke, C. J., & Blanch, H. W. (1999). Protein adsorption at the oil/water
356 interface: characterization of adsorption kinetics by dynamic interfacial tension
357 measurements. *Biophysical Chemistry*, 81(1), 59–80.

358 Chen, B., & O'Mahony, J. A. (2016). Impact of glucose polymer chain length on heat and

- 359 physical stability of milk protein-carbohydrate nutritional beverages. *Food Chemistry*,
360 211, 474–482.
- 361 Chronakis, I. S. (1998). On the molecular characteristics, compositional properties, and
362 structural-functional mechanisms of maltodextrins: a review. *Critical Reviews in Food*
363 *Science and Nutrition*, 38(7), 599–637.
- 364 Douglas, J., Gasoriek, J., Swaffield, J., & Jack, L. (2005). *Fluid Mechanics* (5th ed.). Essex,
365 UK: Prentice Hall.
- 366 Drapala, K. P., Auty, M. A. E., Mulvihill, D. M., & O'Mahony, J. A. (2016). Performance of
367 whey protein hydrolysate-maltodextrin conjugates as emulsifiers in model infant
368 formula emulsions. *International Dairy Journal*, 62, 76–83.
369 <https://doi.org/10.1016/j.idairyj.2016.03.006>
- 370 Fox, P. F. (2008). Chapter 1 - Milk: an overview. In A. Thompson, M. Boland, H. Singh, A.
371 Thompson, & M. Boland (Eds.) (pp. 1–54). San Diego: Academic Press.
- 372 Gonzalez-Perez, S., & Arellano, J. B. (2009). Vegetable protein isolates. In G. O. Philips &
373 P. A. Williams (Eds.), *Handbook of Hydrocolloids* (2nd ed., pp. 383–419). Cambridge,
374 UK: Woodhead Publishing Limited.
- 375 Hall, S., Cooke, M., El-Hamouz, A., & Kowalski, A. J. (2011). Droplet break-up by in-line
376 Silverson rotor–stator mixer. *Chemical Engineering Science*, 66(10), 2068–2079.
- 377 Hall, S., Pacek, A. W., Kowalski, A. J., Cooke, M., & Rothman, D. (2013). The effect of
378 scale and interfacial tension on liquid–liquid dispersion in in-line Silverson rotor–stator
379 mixers. *Chemical Engineering Research and Design*, 91(11), 2156–2168.
380 <https://doi.org/10.1016/j.cherd.2013.04.021>
- 381 Lee, L. L., Niknafs, N., Hancocks, R. D., & Norton, I. T. (2013). Emulsification: Mechanistic

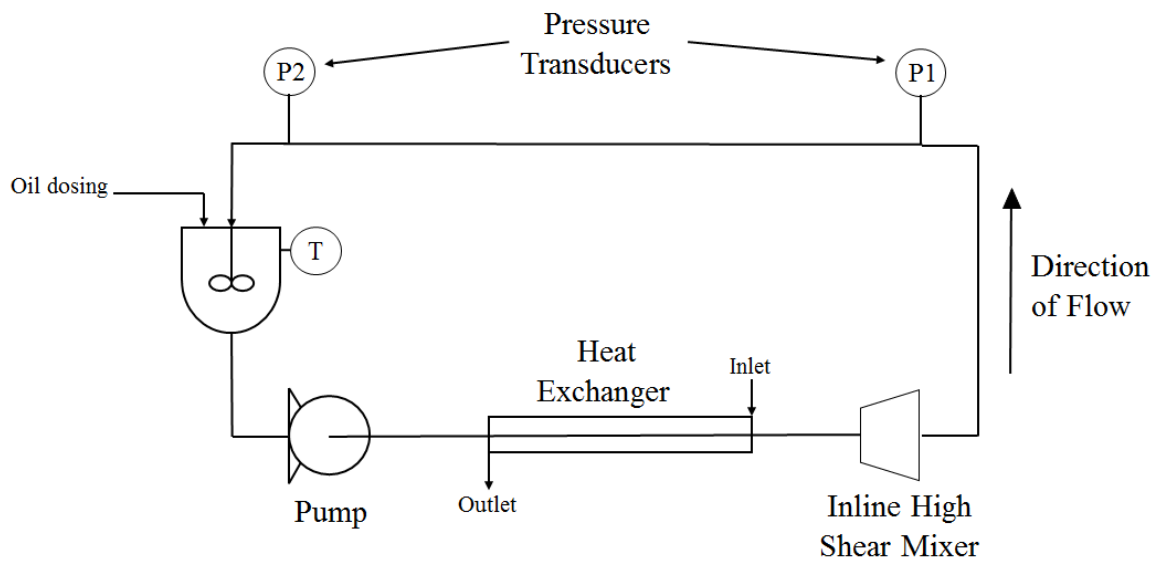
- 382 understanding. *Trends in Food Science & Technology*, 31(1), 72–78.
383 <https://doi.org/10.1016/j.tifs.2012.08.006>
- 384 Lee, L., & Norton, I. T. (2013). Comparing droplet breakup for a high-pressure valve
385 homogeniser and a Microfluidizer for the potential production of food-grade
386 nanoemulsions. *Journal of Food Engineering*, 114(2), 158–163.
387 <https://doi.org/http://dx.doi.org/10.1016/j.jfoodeng.2012.08.009>
- 388 Lerche, D., & Sobisch, T. (2011). Direct and Accelerated Characterization of Formulation
389 Stability. *Journal of Dispersion Science and Technology*, 32(12), 1799–1811.
390 <https://doi.org/10.1080/01932691.2011.616365>
- 391 McClements, D. J. (2005). *Food Emulsions: Principles, Practices, and Techniques* (2nd ed.).
392 CRC Press.
- 393 Mihailova, O., Lim, V., McCarthy, M. J., McCarthy, K. L., & Bakalis, S. (2015). Laminar
394 mixing in a SMX static mixer evaluated by positron emission particle tracking (PEPT)
395 and magnetic resonance imaging (MRI). *Chemical Engineering Science*, 137, 1014–
396 1023.
- 397 Morris, E. R., Cutler, A. N., Ross-Murphy, S. B., Rees, D. A., & Price, J. (1981).
398 Concentration and shear rate dependence of viscosity in random coil polysaccharide
399 solutions. *Carbohydrate Polymers*, 1, 5–21.
- 400 Mulcahy, E. M., Mulvihill, D. M., & O'Mahony, J. A. (2016). Physicochemical properties of
401 whey protein conjugated with starch hydrolysis products of different dextrose equivalent
402 values. *International Dairy Journal*, 53, 20–28.
403 <https://doi.org/10.1016/j.idairyj.2015.09.009>
- 404 O'Connell, J. E., & Flynn, C. (2007). The manufacture and application of casein-derived

- 405 ingredients. In Y. H. Hui (Ed.), *Handbook of Food Products Manufacturing* (1st ed., pp.
406 557–593). New Jersey: John Wiley & Sons.
- 407 O’Mahony, J. A., Drapala, K. P., Mulcahy, E. M., & Mulvihill, D. M. (2017). Controlled
408 glycation of milk proteins and peptides: Functional properties. *International Dairy*
409 *Journal*, 67, 16–34.
- 410 O’Sullivan, J., Arellano, M., Pichot, R., & Norton, I. (2014). The effect of ultrasound
411 treatment on the structural, physical and emulsifying properties of dairy proteins. *Food*
412 *Hydrocolloids*, 42(3), 386–396.
- 413 O’Sullivan, J., Beevers, J., Park, M., Greenwood, R., & Norton, I. (2015). Comparative
414 assessment of the effect of ultrasound treatment on protein functionality pre- and post-
415 emulsification. *Colloids and Surfaces A: Physicochemical and Engineering Aspects*,
416 484, 89–98. <https://doi.org/10.1016/j.colsurfa.2015.07.065>
- 417 O’Sullivan, J. J., & O’Mahony, J. A. (2016). Food Ingredients. In *Reference Module in Food*
418 *Science* (pp. 1–3). Amsterdam, Netherlands: Elsevier.
- 419 O’Sullivan, J. J., Schmidmeier, C., Drapala, K. P., O’Mahony, J. A., & Kelly, A. L. (2017).
420 Monitoring of pilot-scale induction processes for dairy powders using inline and offline
421 approaches. *Journal of Food Engineering*, 197, 9–16.
- 422 O’Sullivan, J., Murray, B., Flynn, C., & Norton, I. (2015). Comparison of batch and
423 continuous ultrasonic emulsification processes. *Journal of Food Engineering*, 167(B),
424 141–121.
- 425 O’Sullivan, J., Murray, B., Flynn, C., & Norton, I. T. (2016). The effect of ultrasound
426 treatment on the structural, physical and emulsifying properties of animal and vegetable
427 proteins. *Food Hydrocolloids*, 53, 141–154.

- 428 O'Sullivan, J., Park, M., & Beevers, J. (2016). The effect of ultrasound upon the
429 physicochemical and emulsifying properties of wheat and soy protein isolates. *Journal*
430 *of Cereal Science*.
- 431 Pacek, A., Baker, M., & Utomo, A. (2007). Characterisation of flow pattern in a rotor stator
432 high shear mixer. In *Proceedings of European Congress of Chemical Engineering*
433 *(ECCE-6)*.
- 434 Pal, R. (1996). Effect of droplet size on the rheology of emulsions. *AIChE Journal*, *42*(11),
435 3181–3190. <https://doi.org/10.1002/aic.690421119>
- 436 Pal, R. (2011). Rheology of simple and multiple emulsions. *Current Opinion in Colloid &*
437 *Interface Science*, *16*(1), 41–60. <https://doi.org/10.1016/j.cocis.2010.10.001>
- 438 Rong, Y., Sillick, M., & Gregson, C. M. (2009). Determination of dextrose equivalent value
439 and number average molecular weight of maltodextrin by osmometry. *Journal of Food*
440 *Science*, *74*(1), C33–C40. <https://doi.org/10.1111/j.1750-3841.2008.00993.x>
- 441 Sharma, A., Jana, A. H., & Chavan, R. S. (2012). Functionality of Milk Powders and Milk-
442 Based Powders for End Use Applications-A Review. *Comprehensive Reviews in Food*
443 *Science and Food Safety*, *11*(5), 518–528. [https://doi.org/10.1111/j.1541-](https://doi.org/10.1111/j.1541-4337.2012.00199.x)
444 [4337.2012.00199.x](https://doi.org/10.1111/j.1541-4337.2012.00199.x)
- 445 Shimoni, G., Shani Levi, C., Levi Tal, S., & Lesmes, U. (2013). Emulsions stabilization by
446 lactoferrin nano-particles under in vitro digestion conditions. *Food Hydrocolloids*, *33*(2),
447 264–272. <https://doi.org/10.1016/j.foodhyd.2013.03.017>
- 448 Vega, C., & Roos, Y. H. (2006). Invited review: spray-dried dairy and dairy-like emulsions--
449 compositional considerations. *Journal of Dairy Science*, *89*(2), 383–401.
450 [https://doi.org/10.3168/jds.S0022-0302\(06\)72103-8](https://doi.org/10.3168/jds.S0022-0302(06)72103-8)

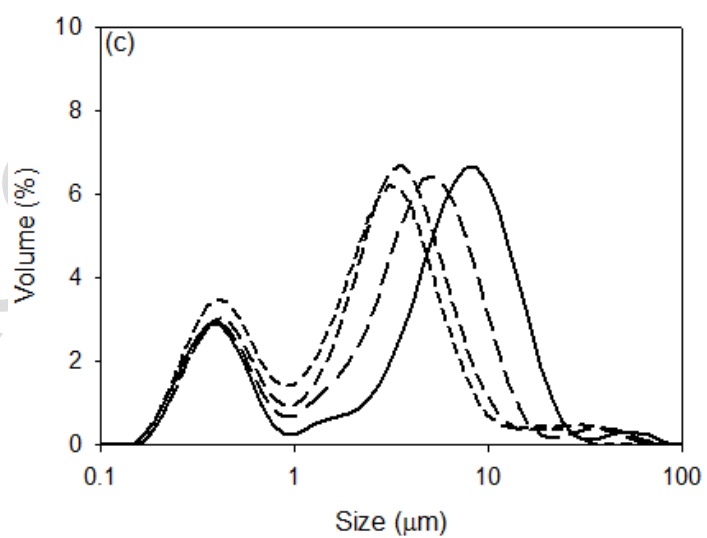
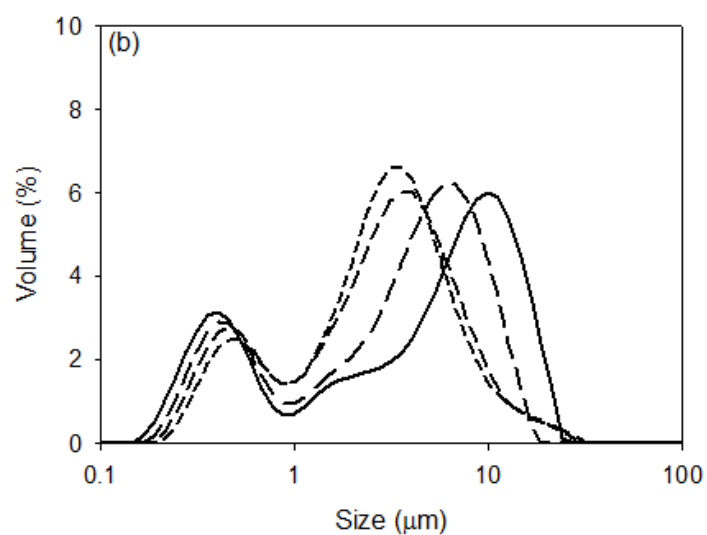
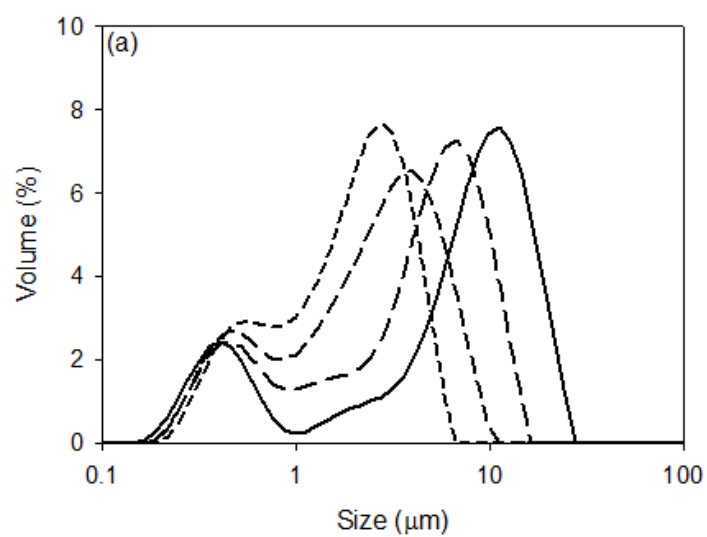
- 451 Vignolles, M.-L., Jeantet, R., Lopez, C., & Schuck, P. (2007). Free fat, surface fat and dairy
452 powders: interactions between process and product. A review. *Le Lait*, 87(3), 187–236.
453 <https://doi.org/10.1051/lait:2007010>
- 454 Vos, B., Crowley, S. V., O’Sullivan, J., Evans-Hurson, R., McSweeney, S., Krüse, J., ...
455 O’Mahony, J. A. (2016). New insights into the mechanism of rehydration of milk
456 protein concentrate powders determined by Broadband Acoustic Resonance Dissolution
457 Spectroscopy (BARDS). *Food Hydrocolloids*, 61, 933–945.
- 458 Walstra, P. (1993). Principles of emulsion formation. *Chemical Engineering Science*, 48(2),
459 333–349. [https://doi.org/http://dx.doi.org/10.1016/0009-2509\(93\)80021-H](https://doi.org/http://dx.doi.org/10.1016/0009-2509(93)80021-H)
- 460 Walstra, P., & Smulders, P. (2000). Emulsion Formation. In B. . Binks (Ed.), *Modern Aspects*
461 *of Emulsion Science* (1st ed., pp. 56–99). Cambridge, UK: The Royal Society of
462 Chemistry.
- 463 Wang, Y.-J., & Wang, L. (2000). Structures and Properties of Commercial Maltodextrins
464 from Corn, Potato, and Rice Starches. *Starch - Stärke*, 52(8–9), 296–304.
465 [https://doi.org/10.1002/1521-379X\(20009\)52:8/9<296::AID-STAR296>3.0.CO;2-A](https://doi.org/10.1002/1521-379X(20009)52:8/9<296::AID-STAR296>3.0.CO;2-A)
- 466

1 Fig. 1.



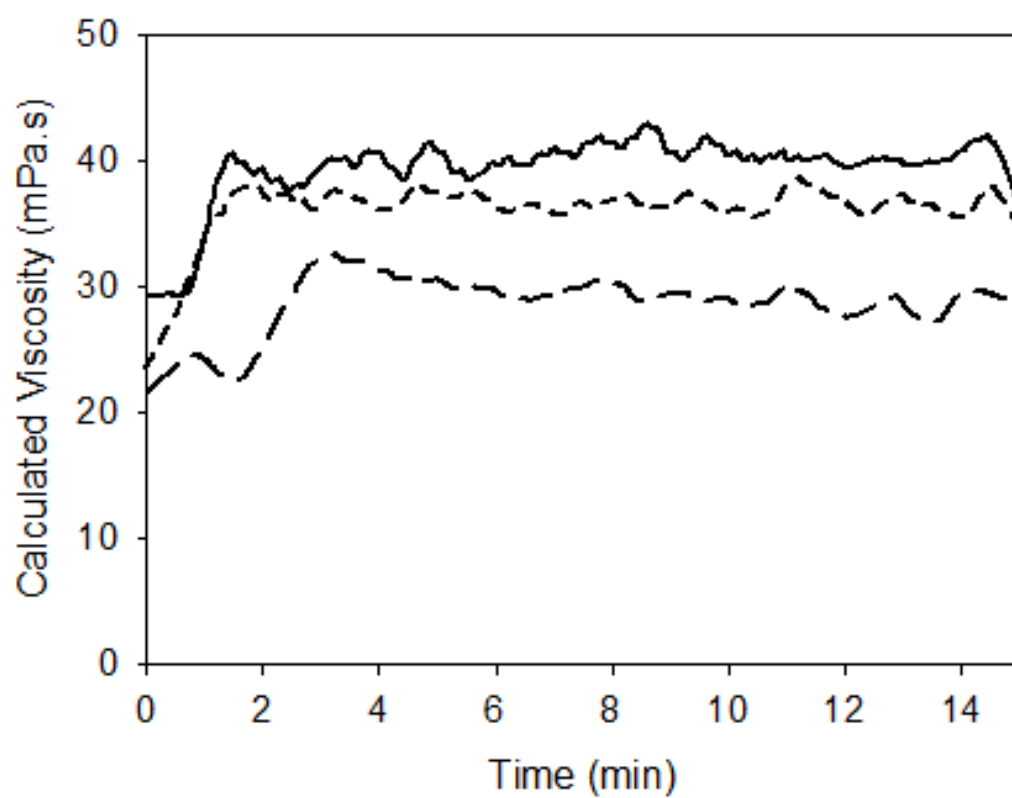
2

1 Fig. 2.



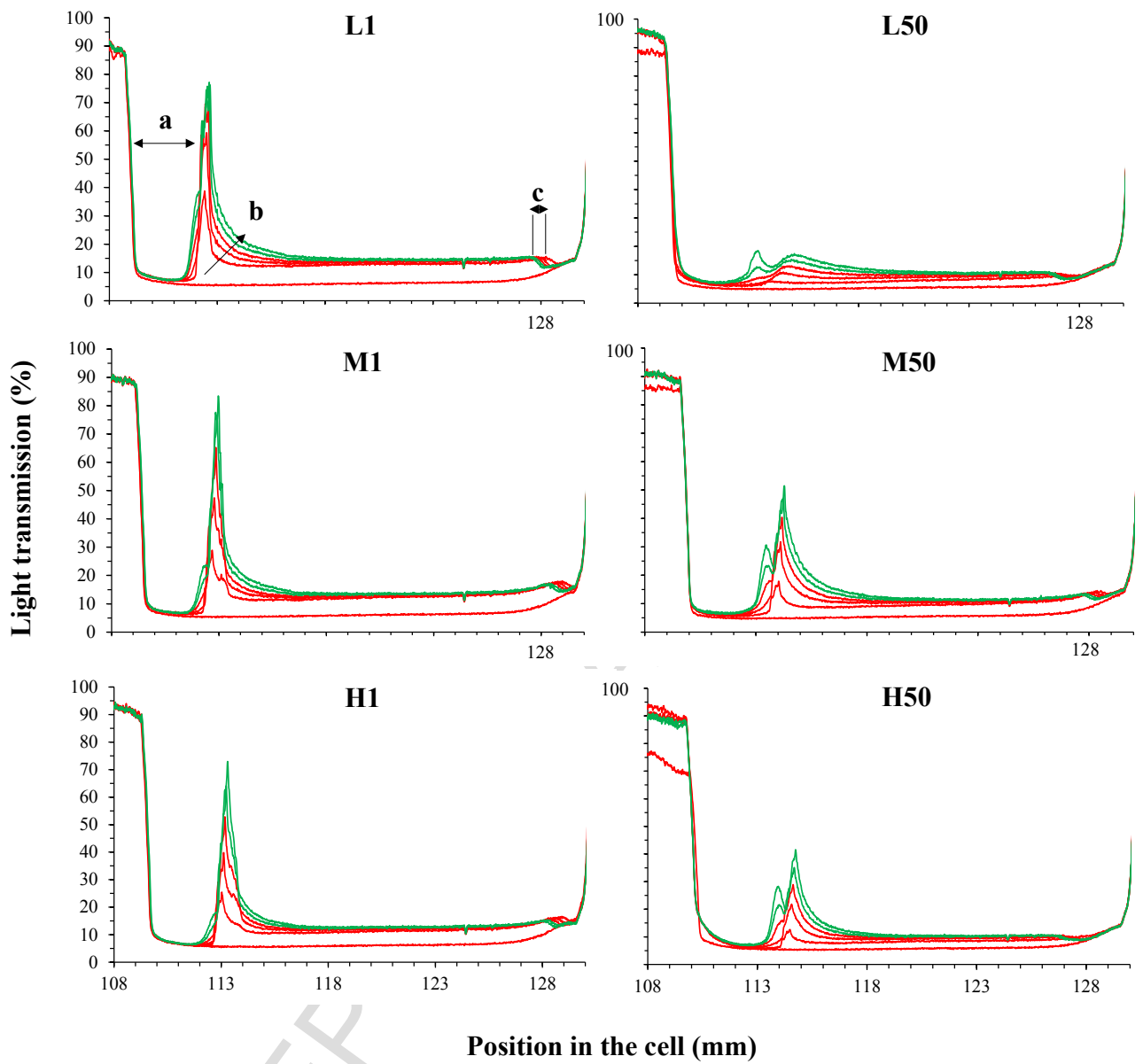
2

1 Fig. 3.

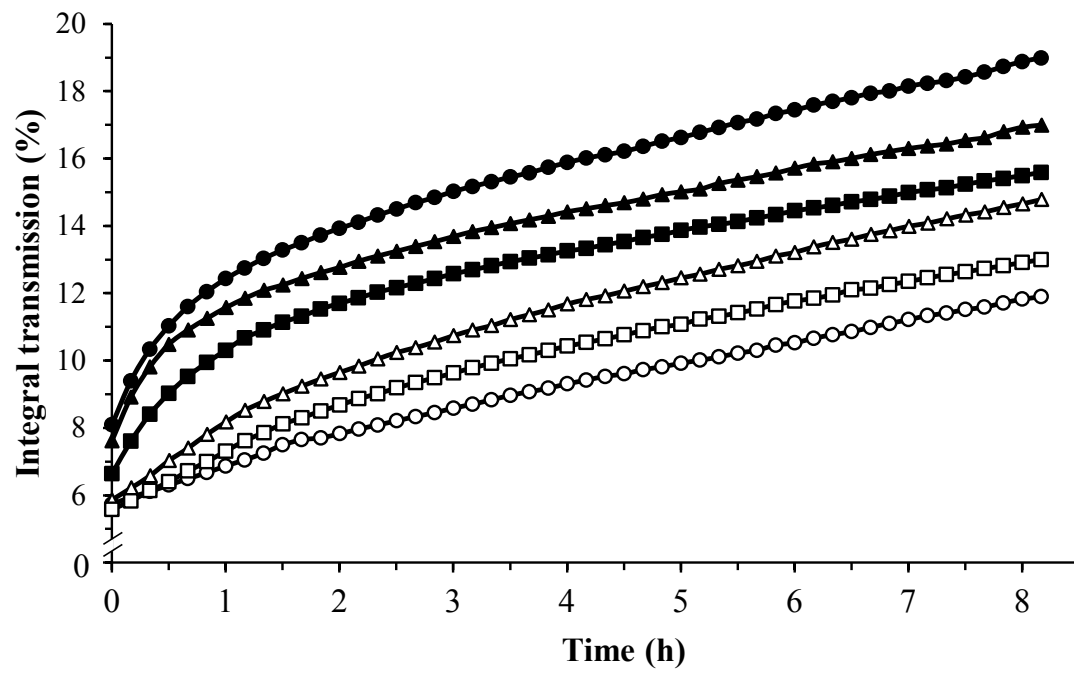


2

1 Fig. 4.

2
3

1 Fig. 5.

2
3

1 **Figure captions**

2 **Fig. 1.** Schematic representation of the experimental configuration employed, showing the
3 inline high-shear mixer, heat exchanger, pressure transducers, batch vessel and pump.

4 **Fig. 2.** Changes in oil droplet size distribution as a function of pass number through the inline
5 high-shear mixer, showing data for 1 (solid line), 5 (long-dashed line), 25 (medium-dashed
6 line), and 50 (short-dashed line) passes after dosing of refined palm oil for: (a) low-protein fat-
7 filled milk emulsions (FFME), (b) medium-protein FFME, and (c) high-protein FFME. The
8 concentration of refined palm oil in all cases was 12% (w/w).

9 **Fig. 3.** Calculated viscosity upon addition of molten refined palm oil to the system as a function
10 of time for low-protein fat-filled milk emulsions (FFME) (solid line), medium-protein FFME
11 (long-dashed line), and high-protein FFME (short-dashed line). The concentration of refined
12 palm oil in all cases was 12% (w/w).

13 **Fig. 4.** Emulsion separation profiles for low- (L), medium- (M) and high-protein (H) fat-filled
14 milk emulsions (FFMEs) after 1 and 50 passes through the inline high-shear mixer. The profiles
15 demonstrate changes in the transmission of light through the sample cell due to migration of its
16 component under centrifugal acceleration. The sample is contained between the position 110
17 mm (top of the cell) and position 129 mm (bottom of the cell). The evolution of the transmission
18 profiles over the duration of the analysis is represented by the arrow (b), where the phase
19 boundary progressively moves towards the bottom of the cell while the thickness of the cream
20 layer increases (a) and the sediment layer builds-up (c). Colours indicate the sequence of the
21 profiles (RED profiles were collected early, first profile at time 0 min; GREEN profiles were
22 collected late in separation, last profile collected at time 500 min – please refer to on-line
23 version for full colour Figure).

24 **Fig. 5.** Separation profiles expressed as integral transmission as a function of time for fat-filled
25 milk emulsions (FFMEs) with low- (circle), medium- (triangle) and high-protein (square) after
26 1 (solid fill) and 50 (no fill) passes through the inline high-shear mixer as measured using the
27 LUMiSizer analytical centrifuge.

1 **Table 1.**

2 Composition of skim milk concentrate (SMC), low-, medium- and high-protein fat-filled milk
 3 emulsions (FFME), and calculated composition of resultant low-, medium- and high-protein
 4 content fat-filled milk powders (FFMP).

	Fat-Filled Milk Emulsions				Fat-Filled Milk Powders		
	SMC	Low	Medium	High	Low	Medium	High
Protein (%)	16.2	7.7	10.5	13	14.2	19.2	23.7
Fat (%)	0.4	12.2	12.2	12	22.4	22.3	22.1
Lactose (%)	23.1	11.4	14.9	18.6	21	27.2	34
Maltodextrin (%)	0	20.3	14.2	8	37.4	26	14.6
Lactose + Maltodextrin (%)	23.1	31.7	29.1	26.6	58.4	53.2	48.6
Ash (%)	1.1	0.5	0.7	0.9	1	1.3	1.6
Water (%)	59.2	47.9	47.5	47.5	4	4	4

5

6 **Table 2.**

7 Effect of pass number (1, 5, 25 and 50) through the inline high-shear mixer on $d_{3,2}$ (*i.e.*, Sauter diameter), $d_{4,3}$ (*i.e.*, volume-weighted mean
 8 diameter), d_{10} , d_{50} , d_{90} , *span*, and separation rates, calculated from the initial linear response ($R^2 \geq 0.95$) of the slope of plots of integral transmission
 9 *vs.* measurement time, for low-, medium- and high-protein fat-filled milk emulsions (FFMEs).

Protein Content (% w/w)	Pass (-)	$d_{4,3}$ (μm)	d_{10} (μm)	d_{50} (μm)	d_{90} (μm)	<i>Span</i> (-)	<i>Rate of initial transmission increase</i> (%/h)
7.7	1	9.62 ± 0.79	0.45 ± 0.01	9.65 ± 0.05	17.4 ± 0.13	1.91 ± 0.02	7.69 ± 0.43
	5	5.47 ± 0.32	0.51 ± 0.01	4.91 ± 0.03	10.5 ± 0.04	2.04 ± 0.01	-
	25	3.08 ± 0.09	0.49 ± 0.02	2.65 ± 0.04	6.35 ± 0.05	2.17 ± 0.03	-
	50	2.31 ± 0.03	0.49 ± 0.03	2.11 ± 0.02	4.41 ± 0.03	1.82 ± 0.02	5.60 ± 0.05
10.5	1	6.67 ± 0.31	0.43 ± 0.04	5.76 ± 0.07	16.8 ± 0.09	2.89 ± 0.05	6.85 ± 0.35
	5	4.89 ± 0.08	0.51 ± 0.05	3.73 ± 0.04	12.3 ± 0.02	3.16 ± 0.02	-
	25	4.05 ± 0.02	0.52 ± 0.03	2.83 ± 0.02	8.21 ± 0.05	2.73 ± 0.01	-
	50	3.99 ± 0.06	0.65 ± 0.03	2.82 ± 0.01	6.85 ± 0.06	2.26 ± 0.02	5.47 ± 0.03
13	1	9.41 ± 0.87	0.37 ± 0.01	6.58 ± 0.09	15.4 ± 0.13	2.34 ± 0.06	6.16 ± 0.07
	5	6.22 ± 0.51	0.39 ± 0.01	4.15 ± 0.04	10.8 ± 0.05	2.42 ± 0.08	-
	25	4.52 ± 0.31	0.41 ± 0.01	3.04 ± 0.02	8.11 ± 0.07	2.57 ± 0.05	-
	50	3.74 ± 0.19	0.36 ± 0.01	2.52 ± 0.04	7.09 ± 0.06	2.74 ± 0.11	5.35 ± 0.12

11 **Table 3.**

12 Comparison of calculated viscosity (1 and 50 passes after dosing of molten refined palm oil)
 13 and experimentally measured viscosity (at a shear rate of 300 s^{-1}) for fat-filled milk emulsions
 14 with low-, medium- and high-protein contents. The concentration of refined palm oil in all
 15 cases was 12% (w/w).

Number of Passes (-)	Protein Content (% w/w)	$\eta_{\text{calculated}}$ (mPa.s)	$\eta_{\text{experimental}}$
1	7.7	29.1 ± 1.1	22.6 ± 0.2
	10.5	21.8 ± 0.8	13.5 ± 0.5
	13	23.9 ± 1.7	26.5 ± 2.9
50	7.7	36.5 ± 1.3	33.4 ± 0.5
	10.5	29.2 ± 0.7	15.9 ± 1.5
	13	34.7 ± 2.2	27.6 ± 3.2

16